The evolution of pectate lyase-like genes across land plants, and their roles in haustorium formation in parasitic plants

Authors: Huiting Zhang[1,2], Eric Wafula[1], Elizabeth Kelly[1,2], Itsuhiro Ko[3], Alan Yocca[1], Pradeepa Gunathilake[4], Zhenzhen Yang[1,2], John Yoder[5], Loren Honaas[6], Claude dePamphilis[1,2]*

Author affiliations:

1. Department of Biology, the Pennsylvania State University, University Park, PA, USA
2. The Plant Biology Program, Huck Institute of Life Sciences, the Pennsylvania State University, University Park, PA, USA
3. Plant Science, College of Agriculture, the Pennsylvania State University, University Park, PA, USA
4. Agricultural Biotechnology Center, University of Peradeniya, Peradeniya, Sri Lanka
5. Department of Plant Sciences, UC Davis, Davis, CA, USA
6. Physiology and pathology of tree fruit research unit, USDA ARS, Wenatchee, WA, USA

*Corresponding author: Claude dePamphilis

Abstract

Parasitic plants in the Orobanchaceae family are noxious agricultural pests that severely impact crops worldwide. These plants acquire water and nutrients from their hosts through a specialized organ called the haustorium. A critical process in the formation and function of the haustorium involves cell wall modification. In this study, we identified and analyzed the evolutionary relationships of *pectate lyase-like* (*PLL*) genes in parasitic plants and other major land plant lineages. One particular *PLL* gene, denoted as *PLL1* in parasitic Orobanchaceae, which our previous research identified as a potential key parasitism gene, belongs to the largest sub-clade of this gene family. To explore the role of *PLL1* gene in parasitic Orobanchaceae further, we manipulated its transcript abundance during haustorium development in *Triphysaria versicolor*, a model species in parasitic Orobanchaceae, using both direct transformation of the parasite and host-induced-gene-silencing (HIGS). For HIGS, we generated transgenic hosts (*Medicago truncatula* and *Arabidopsis thaliana*) carrying hairpin RNAs targeting the *PLL* gene in *T. versicolor*. Our results demonstrated that both methods effectively reduced the *PLL1* expression in the haustorium of *T. versicolor*, leading to an increase in poorly adhered parasites. These findings highlight *PLL1*'s crucial role in haustorium development in Orobanchaceae and may inform novel strategies towards parasitic weed management.

Introduction

Pectins, a family of complex polysaccharide polymers, are major components of primary cell walls and the middle lamellae of land plants. In higher plants, pectin functions in maintaining the mechanical and structural integrity of plant cell walls, contributes to intercellular adhesion [1], and plays a role in plant defense [2,3]. Several classes of pectin degrading enzymes have been identified in bacteria, fungi, and plants. One of those is pectate lyase (PL), an enzyme that cleaves the α-1,4-linked galacturonic acid in homogalacturonan by beta-elimination. PLs have been well documented in plant pathogens such as *Erwinia carotovora* and *Bacillus* spp. as extracellular pathogens in soft rot disease [4–6]. In plants, *pectate lyase-like* genes (*PLLs*) play essential roles in various developmental and reproductive processes. During pollen tube growth, *PLL* functions by loosening pollen cell walls to initiate pollen tube emergence [7–10]. Plant *PLLs* are also involved in the activation of plant defenses by releasing plant cell wall oligogalacturonides as defense elicitors in response to various plant hormones and stresses [11]. In addition, *PLLs* studies in horticulture crops revealed their roles in the development of important crop traits [12]. *GhPEL76*, a *PLL* gene in cotton, regulates the organ elongation in Arabidopsis and fiber elongation in cotton [13]. Gene silencing

assays in tomato and peach shed light on the roles that *PLLs* play in fruit ripening and softening [14,15].

Haustoria, the feeding structures that are present in all parasitic plants, are evolutionarily novel organs in the plant kingdom. Several studies have shown that parasitic plants have recruited haustorial genes from ancestral genes function in nonparasitic plant tissues to adapt to a parasitic lifestyle [16–18], including those involved in pectin modification and degradation processes [17,19–25]. One such example is the *PLL* gene family [17]. In a study conducted by Yang *et al*., comparison between *PLL* gene expression patterns in the parasites and their orthologs in nonparasitic plants in Orobanchaceae suggested that ancestral genes in parasitic plants were commonly expressed in floral tissues and that the haustorial expression was gained through regulatory neofunctionalization after a genome duplication event [17]. Haustorial specific *PLL* genes from three parasitic species in Orobanchaceae were proposed to be good candidates for functional assays [17] and could be potential genetic engineering targets for parasitic weed management [26]. Dynamic regulations of cell wall modification enzymes, including PLLs, were also observed in another parasitic plant, *Cuscuta*, during haustorium development and parasite-host interaction [23–25].

Unlike functional characterization in model plant species where high-efficiency protocols have been developed and tested exhaustively, functional assays in parasitic plants remain a challenging endeavor. A method was proposed by Zhang 2020 [27], to select the best candidate genes for functional analysis in non-model organisms using a combination of transcriptome data, gene family phylogeny, and molecular evolution tests. To qualify for a good candidate gene, more analyses are need on the parasitic plant *PLL* genes, such as validation of gene models, analysis of gene expression patterns on a uni-gene level, and identification of paralogous genes that might have functional redundancy; all of which can be facilitated with a gene family analysis. However, a comprehensive view of the evolutionary history of the PLL family is lacking. Sun and van Nocker used the Neighbor-Joining method to construct a *PLL* family phylogeny in Arabidopsis [28], which served as the baseline for more detailed phylogenetic studies of *PLLs* across land plants [29,30] or for a specific lineage [14,31]. In the aforementioned cases, however, only a limited number of species were selected and the phylogenetic relationships between some large groups remains unresolved or lacks strong support. Additionally, phylogenetic relationships from those studies conflict each other. To gain a deeper understanding of the evolutionary history of the *PLL* gene family in plants, especially in parasitic plants, and to verify whether the *PLLs* identified by Yang *et al.* meet the requirement of good candidate genes for functional studies, a well resolved phylogeny across a wide range of plants is needed.

In this study, with a goal of investigating the evolution of *pectate lyase-like* genes in parasitic plants and examining the involvement of *PLLs* in haustorium development,

we implemented a phylogenetic approach to study the *PLL* gene family across land plants and gene knockdown assays on a selected *PLL* gene in parasitic plants. A haustorially expressed *Triphysaria versicolor PLL* gene, *TrVeBC3_16311.1*, designated as *TrVePLL1*, was selected for functional assays in the model parasitic plant *T. versicolor*. Both transient transformation via hairy root transformation [32,33] and host induced gene silencing (HIGS) assays [34] were used to knockdown the expression of the target gene. Knockdown assays resulted in fewer mature haustoria and weakened haustorial connections, demonstrating the involvement of *TrVePLL1* in plant parasitism and indicating that the HIGS knockdown strategy could contribute to parasite control in agriculturally damaging parasites.

Materials and methods

Pectate-lyase like gene identification and phylogenetic inference

The following processes were accomplished using the PlantTribes2 [35] tools in Galaxy (https://usegalaxy.org/) [36], following the method from Zhang et al. [37].

Genes (*Arabidopsis PLL* genes), genomes (*Cuscuta* spp., *Ipomoea* spp., *Lindenbergia philippensis*, and *Striga hermonthica*), or transcriptomes (*T. versicolor* build 4, *S. hermonthica* build 4, *P. aegyptiaca* build 6, and *L. philippensis* build 2) of interest were processed to predict protein coding regions using *AssemblyPostProcessor* with TransDecoder [38]. A list of genomes and transcriptomes and data source can be found in Supplemental Table S1. The post-processed sequences were classified to into the pre-computed orthologous gene family clusters (orthogroups) of the 26Gv2.0 scaffold from PlantTribes2 with *GeneFamilyClassifier* using both BLASTp [39] and HMMER hmmscan [40] . The classified sequences were then assigned with the corresponding orthogroups' metadata including functional annotation and super orthogroup assignment. Annotations of orthogroups within the same super orthogroups under certain classification stringency were investigated to identify missing *PLL* genes. A total of four orthogroups were identified as *PLLs* from the PlantTribes2 26Gv2.0 scaffold (Supplemental Table S2)

Sequences classified into desired orthogroups were integrated into the scaffold gene models using the *GeneFamilyIntegrator* tool and then all merged into one fasta file for downstream process. Multiple sequence alignments were generated using *GeneFamilyAligner* using MAFFT's L-INS-i algorithm [41] and the corresponding coding sequences were forced onto the amino acid alignment. Sites present in less than 10% of the aligned DNA sequences, and sequences with less than 50% alignment coverage were removed with trimAL [42]. Maximum likelihood (ML) phylogenetic trees were

estimated from the trimmed DNA alignments using two programs. First, a RAxML tree [43] was constructed using the PlantTribes2 tool *GeneFamilyPhylogenyBuilder* with 1000 bootstrap replicates to estimate the reliability of the branches on the trees. Second, IQtree2 [44] was used to infer phylogenetic trees with 2000 ultrafast bootstrapping and the -bnni flag for UFBoot tree optimization [45]. In addition, *PLL* gene family trees with sequences from only autotrophic plants were constructed using the same methods after removing parasitic plant sequences.

Monophyletic clades from all the four phylogenetic trees were identified and named following the convention proposed in the Sun and van Nocker, 2010 research. Genes belonging to each clade were compared across the four trees (Supplemental Table S3). Because all the four trees share the same clade topology and almost the same genes were present in each clade, the IQtree constructed phylogenies were used for downstream analysis due to higher bootstrap support values.

Manual curation of parasitic plant *PLL* genes

The putative *Triphysaria versicolor PLL* transcripts were subject to manual curation with webAUGUSTUS [46] (https://bioinf.uni-greifswald.de/webaugustus/, last accessed: May 7th 2024). A BLASTn search was performed on each transcript against the *T. versicolor* 10X genome assembly to identify the genomic region corresponding to the *PLL* transcript. A genomic fragment containing the target transcript and 3kb upstream and downstream of the targeting region was extracted as the *genome file* input. Next, a BLASTp search was performed on the protein sequence predicted from each transcript against the protein sequences from the PLLs identified from the previous step. Sequences with the highest bitscore from closely related species (*Striga asiatica*, *Mimulus guttatus*, *Lindenbergia philippensis*, and *Solanum lycopersicum*) and Arabidopsis were selected as the *cDNA evidence file* input. *Solanum lycopersicum* was selected as the model organism for AUGUSTUS *species* parameters. Genes from both strands were reported and analyzed. Full length genes were identified by aligning the post-processed transcript, gene models predicted by AUGUSTUS, and the reference sequences used as cDNA evidence for AUGUSTUS prediction. For cases while AUGUSTUS default setting failed to predict full length genes, the transcript(s), predicted exons, and *Striga asiatica* gene were mapped to the *T. versicolor* 10X genome assembly and the coding region were manually determined by using *S. asiatica* gene as a reference. Surprisingly, the *TrVeBC3_16311.1* gene identified by Yang et al., 2015 was missing in the *T. versicolor* transcriptome build 4. Manual annotation using the method described above was able to recover this gene from the genome assembly and seven exons were identified. The same method was used to improve *Cuscuta campestris* gene models, with *C. australis* and *Ipomea* orthologs as reference.

Domain prediction and amino acid frequency analysis

Domain structures of proteins in each clade were predicted using the command line version InterProScan (v5.59.91) [47] and searched against all the databases. To predict the presence of transmembrane domains and signal peptides, the protein sequences were submitted to the SignalP-5.0 [48] server and TMHMM server v2.0 [49] under default settings.

The Pec_lyase_C domains predicted in each sequence by Interproscan were isolated and a MAFFT alignment was performed on the coding sequences comprising the focal domain. Sequences from the same clade identified from the gene family phylogenetic tree were extracted from the alignment and submitted to WebLOGO (https://weblogo.berkeley.edu/logo.cgi, last accessed: May 8th 2024) [50] to create the amino acid frequency plot.

Selective constraint analysis

To infer adaptive or purifying selection, the EasyCodeML software (v1.21) [51] was used to perform hypothesis testing using the CodeML program [52] from the PAML package. Since some gene relationships were not clear in the full phylogenetic tree, genes from each clade and subclade were extracted and clade/ subclade trees were constructed using the same method as described above. Sub-trees are available in Supplemental File 1. Branches housing parasitic plant *PLL* genes and some non-parasitic asterid genes were identified from the subtrees and subjected to the test (Supplemental File 2). The branch-model in CodeML was first tested in the clades with parasitic plant *PLL* genes using the present parameters (nested models). The parasite genes were selected as foreground and the rest were identified as background. A likelihood ratio test was performed afterwards to determine whether the branch model (M2) fits better than the one ratio model (M0). For the cases when the branch model fits significantly better than the one ratio model, a branch-site test was performed to identify sites under positive selection for the indicated foreground lineages. The preset (nested models) parameters were used to perform the branch-test and the same branches were selected for this test as were used in the branch model. The Bayes empirical Bayes (BEB) method [53] was used to identify amino acids that are evolving under selection.

Plant material

Seeds of *Triphysaria versicolor* were obtained from the Yoder lab at University of California, Davis. *Arabidopsis thaliana* Columbia-0 seeds were obtained from the Anderson lab at the Pennsylvania State University (PSU). *Medicago truncatula* Jemalong A17 seeds were kindly provided by David Stout from USDA Agricultural Research Service, Pullman, WA and propagated in the Buckhout greenhouse at PSU.

Seed germination: *T. versicolor* seeds were surface sterilized with 70% ethanol for 10 min with shaking and then washed twice with distilled water. Next, seeds were scarified with *Triphysaria* sterilization solution (50% household bleach, 0.01% Triton X-100) for 30 min. on a platform shaker with the speed of 95 rpm and then washed twice with distilled water. The treated *T. versicolor* seeds were transferred to petri dishes with plant growth medium (1/4 x Hoagland's basal salt and nutrient mix, 7.5 g/L plant tissue culture grade agar, pH of 6.1), and sealed with Micropore (3M) surgical tapes. Seeds were allowed to stratify for 3 days at 4°C in the dark. Seeds were then incubated in a 16°C growth chamber with a 12-hour light regime under 30 μmoles photons/m^2/sec light intensity. *M. truncatula* seeds were scarified by soaking in 18M H_2SO_4 for 8 min. with gentle stirring every 2 min. After the seeds were thoroughly washed with reverse osmosis water five times, they were sterilized with *Triphysaria* sterilization solution for 5 min. with gentle shaking. The sterilized seeds were then washed with distilled water 10 times. Scarified and sterilized seeds were transferred to a new tube with 20 ml distilled water and incubated on a shaker with gentle agitation at room temperature for 6 hours to overnight. Water was decanted after the incubation period and seeds were left in the tubes to grow in the dark for 12-24 hours at room temperature. The germinated seeds were transferred to petri dishes with the same growth medium used for *T. versicolor* and incubated in a growth room at 25°C with a 16-hour light regime under 100 μmoles photons/m2/sec light intensity. *A. thaliana* seeds were sterilized using 30% bleach with 0.1% SDS for 20 min., and shaken with a vortex shaker every 10 min. The sterilized seeds were washed with distilled water five times and transferred to petri dish containing MS growth medium (1/2 x Murashige and Skoog basal salt mixture, 10g/L sucrose, and 8g/L plant tissue culture grade agar, pH of 5.7). The treated seeds were incubated in a 22°C growth chamber with a 16 hour light period.

Parasite and host co-culture: *M. truncatula* and *A. thaliana* plants with robust root systems were transferred to co-culture medium (1/4 x Hoagland's basal salt and nutrient mix, 7.5 g/L sucrose, 7.5 g/L plant tissue culture grade agar, pH of 6.1). Host roots were carefully arranged approximately along the radius of the 150 mm petri dish. *Triphysaria* root tips were placed 0.5-1 mm from the host roots. Co-culture plates were sealed with Micropore (3M) surgical tape and placed on growth racks with a 10 degree angle from level. The growth racks were incubated in a growth room at 25°C with a 16-hour light regime under 100 μmoles photons/m2/sec light intensity until tissue collection.

Haustorium development assay and tissue collection

To track changes in *TrVePLL1* expression levels during haustorium development, wild type *Triphysaria versicolor* was co-cultured with *Medicago truncatula* for up to 10 days. Haustorium tissue was collected at 12, 24, 48, 72, 120, and 240 hours post inoculation (HPI). Pre-attachment haustoria (at 12 and 24 HPIs) were collected by making

cuts adjacent to the swollen region of the parasite roots. The post-attachment haustoria (48-240 HPI) were harvested by making cuts in both the parasite and host roots within 1mm adjacent to the haustoria. Harvested tissue was immediately frozen in liquid nitrogen and stored in -80C until processing.

Plasmid construction

To construct the hairpin RNAi vector, a 503-nucleotide region towards the 3' end of the *TrVePLL1* open reading frame was amplified with primers containing four nucleotides, CACC, at the 5' end of the forward primer. The PCR product was recombined into the pENTR™/D-TOPO® entry vector using the pENTR™ Directional TOPO® Cloning kit (Invitrogen) following the manufacturer's protocol. The entry construct was confirmed by Sanger sequencing and sequence comparison with the reference. Next, a Gateway® LR recombination reaction was performed to transfer the target amplicon into the pHG8-YFP parent vector facilitated by Gateway® LR Clonase® II enzyme mix (Invitrogen). A double enzymatic digestion with restriction endonucleases XbaI and XhoI was performed to screen for positive hairpin vectors. The selected vector is named *pHpTvPLL1* and was transformed into *Agrobacterium rhizogenes* strain MSU440 via electroporation. Primer sequences can be found in Supplemental Table S4.

Hairy root transformation

Triphysaria versicolor transformation process was performed following Bandaranayake and Yoder, 2018 [54] with modifications. *Agrobactrium rhizogenes* was grown on mannitol-glutamic acid: Luria-Bertani (MG/L) medium containing 400 uM acetosyringone (Sigma-Aldrich) overnight or until the bacteria covered the petri dish and formed a thick lawn. Ten to fifteen-day old *Triphysaria* seedlings were used for transformation. A clear cut was made at the joint between the hypocotyl and the root. The wounded hypocotyl end of the seedling was dipped into the *A. rhizogenes* culture several times. Petri dish containing MS medium with 3% sucrose was treated with freshly prepared acetosyringone at the concentration of 400 uM. The *A. rhizogenes* infiltrated plantlets were transferred onto the aforementioned plates and then incubated vertically in a 16°C growth chamber with a 12-hour light regime under 30 µmoles photons/m^2/sec light intensity for 7 to 10 days. To initiate root growth, plantlets were transferred to new growth medium (1/4 x Hoagland's basal salt and nutrient mix, 7.5g/L sucrose, 7.5 g/L plant tissue culture grade agar, pH of 6.1) with 300 uM Timentin and incubated for

another 14 days. Transgenic calli and roots were identified by the visualization of YFP fluorescent signal using Zeiss SteREO Discovery.V12 with X-Cite® series 120 Q lamp under a YFP filter. Non-transgenic calli were discarded and non-transgenic roots were removed. Plants with positive signals were moved to a new growth medium and the tips of the transgenic roots were trimmed to allow proliferation. Plates containing the transgenic plants were incubated vertically in a growth room at 25°C with a 16-hour light regime under 100 µmoles photons/m2/sec light intensity. Plants were screened and transferred to a new medium every 2 to 3 weeks until used for co-culture experiments.

Host plants, *i.e. Medicago truncatula* and *Arabidopsis thaliana*, transformations were performed following Biosson-Dernier et al., 2001 [55] with modifications. *A. rhizogenes* were prepared as described above. *Medicago* seeds were germinated as described above and seedlings grown in the dark for 36-48 hours were used for transformation. Arabidopsis seedlings with expanded cotyledon were used for transformation. To make a wound in the host plant seedling, a cut was made about 2-3 mm from the tip. The wounded plant was dipped in the *A. rhizogenes* culture and then transferred to growth medium (1/4 x Hoagland's basal salt and nutrient mix, 7.5 g/L plant tissue culture grade agar, pH of 6.1) treated with freshly made acetosyringone at the concentration of 400 uM. The plates were placed vertically in the 16°C growth chamber for 5 days and transferred to fresh plates and incubated in the 25°C growth room. Transformed plants were subject to YFP screening 2 weeks post infiltration. Plants with no transgenic signal were discarded and roots with no YFP signal were removed with a scalpel. Plants were screened and transferred to a new medium every 2 to 3 weeks until used for co-culture experiments. Arabidopsis was only used as the host plant for Triphenyl tetrazolium chloride staining assay, as described below, while *M. truncatula* was used as the host plant for all the other experiments.

Haustorium categorization and tissue collection

To test the effect of *PLL* knockdown on haustorium development, co-culture experiments were performed on the following parasite-host pairs: 1) *T. versicolor* transformed with *pHpTvPLL1* and co-cultured with wild type host; 2) *T. versicolor* with *pHG8-YFP* (empty vector control) co-cultured with wild type host; 3) Wild type *T. versicolor* co-cultured with host plant transformed with *pHpTvPLL1*; 4) Wild type *T. versicolor* co-cultured with host plant transformed with *pHG8-YFP* (empty vector control). Parasite-host co-cultures were monitored daily. Parasite root tips that started haustorial initiation later than 24 hours post inoculation were marked and not taken into consideration in the final analyses. Transgenic *Triphysaria* roots were allowed to grow in the presence of a wild type host for 7 days before harvesting. Two-week-old *Triphysaria* seedlings were allowed to grow in the presence of a transgenic host root for 5 days before collection. A gentle force was applied to the haustorium: host root was secured

with one pair of tweezers and parasitic root adjacent to the haustorium was pulled gently. Haustoria that breaks easily from the host root with the gentle force were categorized as 'failed' haustoria, while the rest were categorized as 'mature' haustoria. When counting root tips forming mature or failed haustorium, in order to account for human bias, a random number was assigned to each co-culture plate and the researcher recorded the haustorium type without knowing the treatment of each plate.

Five or six biological replicates were created for each co-culture pair. For transformed *T. versicolor* and wild type host co-culture, 50-60 transgenic roots from 8-10 independent *T. versicolor* root cultures were used in each biological replicate. For wild type *T. versicolor* and transgenic host co-culture, 80-100 *T. versicolor* seedlings were inoculated onto 8-10 transgenic host roots in each biological replicates. A Student's t-test was performed on knockdown versus vector control co-culture experiments on the percent of mature / failed haustoria. The co-culture and haustorium categorization assays were performed two more times at a smaller scale. Results from the three experiments are summarized in Supplemental Table S5.

The failed haustoria were collected using the same methods for collecting pre-attachment haustoria. The mature haustoria were harvested using the same method for harvesting post-attachment haustoria. To test the presence of transformed DNA fragments in the host roots, *M. truncatula* roots (transformed roots with or without YFP signal and wild type roots) were collected by cutting the whole root from the plant. Three biological replicates were transferred immediately to liquid nitrogen for nucleic acid isolation, and the rest were transferred immediately to staining/ fixation solutions for staining assays.

Nucleic acid isolation

Haustorial tissues collected for RNA isolation were ground in 350 ul RA1 buffer (Macherey-Nagel) mixed with 1% beta-mercaptoethanol (Qiagen) using Kimble Chase glass tissue grinders (part# KT885450-0020). Total RNA was isolated using the Macherey-Nagel NucleoSpin® RNA Plant kit following the instructions from the user manual (section 5.1). Medicago root tissue collected for DNA isolation were ground in liquid nitrogen and DNA isolated using the Macherey-Nagel NucleoSpin® Plant II kit following instructions in section 5.1 from the user manual. Concentrations of the extracted DNA and RNA samples were assessed on the Qubit fluorometer (Thermo Fisher Scientific) using dsDNA BR (broad range) Assay Kit and RNA HS Assay Kit, respectively.

Haustorium staining assays

Three staining assays were deployed to examine morphological changes within the haustoria formed from the transgenic root and the control roots. Triphenyl tetrazolium chloride (TTC) staining was performed to observe metabolic activities in the haustoria [56]; Toluidine blue O (TBO) staining was performed to investigate changes in cell wall component in the haustoria [57]; Ink-vinegar staining was performed to visualize xylem bridges and other internal features of the haustorium.

TTC staining was performed following Porter et al., 1947 [58] with modifications. *Medicago* root accumulates red or green pigments in co-culture conditions, therefore, *Arabidopsis* was used in this experiment instead. 1% tetrazolium solution was prepared and stored at 4°C in the dark. Haustoria connected to the same host root were collected together and immediately transferred to a 50ml falcon tube containing 30 ml of 1% tetrazolium solution. The plant tissue was immersed in tetrazolium solution and then incubated at room temperature in the dark for 24 hours before screening. Zeiss SteREO Discovery.V12 was used to visualize the staining result and capture images.

TBO staining was performed on haustoria infiltrated with 4% paraformaldehyde. The Leica TP1020 - automatic tissue processor at PSU Core Facility was used to dehydrate and infiltrate the tissue with paraffin (process described in Supplemental table S6). One to several haustoria were embedded in a paraffin mold with the host root oriented on the vertical axis using the Leica EG 1150C tissue embedding workstation. Sections with the thickness of 8um were made with a rotary microtome (Thermo Fisher Scientific) and de-waxed with a Leica autostainer XL with program 3 (Supplemental table S6). TBO solution was added to regions on the slides where tissue was present and incubated at room temperature of 30 seconds. Slides were cleaned with distilled water. Stained slides were visualized and images were captured with an Olympus BX61 microscope.

Ink-vinegar staining of the haustoria was performed following Vierheilig et al., 1998 [59] with modifications. Host roots harboring one to several haustoria were collected in tissue embedding cassettes and placed in glass staining dishes with clearing solution (10% KOH solution). Samples were incubated at room temperature for 4 to 5 days and examined under dissecting scope daily to determine whether the clearing process was completed. Once the tissue is clear, cassettes were moved to a large stainer and rinsed in cold running water for 5 min. The cassettes were then submerged in acidified water (5% white vinegar) for 5 min and rinsed briefly under cold tap water. The cleared and rinsed samples were placed in a preheated 5% ink solution in a water bath at 90°C for 30 min. Cassettes were removed to allow staining solution to drain, and then cassettes were rinsed under cold running water until water runs clear. Stained samples were moved to sterilized acidified water overnight to remove excessive ink

staining. Samples were visualized and images were captured with Zeiss SteREO Discovery.V12.

Transcript level analyses

cDNA was synthesized from RNA used for transcriptome sequencing in the PPGP project [17] or RNA collected for this project. 200 nanograms of RNA from each sample were converted to cDNA using the AzuraQuant™ cDNA Synthesis Kit (Azura Genomics).

Primers for transcript level measurement were designed using Primer3 (v. 0.4.0, http://bioinfo.ut.ee/primer3-0.4.0/) [60,61]. To test primer specificity, melting curve analysis was performed on each PCR reaction and primer pairs yielding more than one peak in the melting curve were not used.

The reverse transcription products were diluted 10-fold, and 1ul was used for each the qRT-PCR reaction with PerfeCTa SYBR Green FastMix (QuantaBio). The reaction was performed with StepOnePlus Real-Time PCR System (Thermo Fisher Scientific) with the following program: Step 1. 95°C for 5 min.; Step 2. 95°C for 0.5 min.; Step 3. 60°C for 0.5 min.; Repeat Step 2 and 3 for 40 cycles; Melt curve: 0.5 increments from 95°C to 25°C.

The average crossing point (Ct) values from three technical replicates were used to represent each biological replicate and three biological replicates were measured for each sample. The 2^(-ddCt) method was used to calculate the fold change in expression of target genes relative to the constitutively expressed gene *TrVePP2A*. Due to low replicate numbers (three replicates), Mann-Whitney-Wilcoxon (MWW) test was performed to test whether there is a significant difference in the expression level of *TrVePLL1* in the control versus the knockdown lines.

Results

Phylogenetic analysis of the pectate lyase-like gene family across land plants

Maximum Likelihood (ML) trees with genes from autotrophic species across land plants and from autotrophic plus parasitic plants (a list of selected species are listed in Supplemental Figure S1) were constructed. The autotrophic plant-only tree was created because some parasitic plant sequences are less well annotated and may possess highly divergent nucleotide sequences due to their unique life-style, thus affecting tree structure and node support. To increase taxon sampling as well as provide comparison between parasites and closely related autotrophs, genes from four high quality genomes (*Ipomoea nil [62]*, *I. trifida [63], and Lindenbergia philippensis;* representing the

nonparasitic sister group of the parasitic Convolvulaceae and Orobanchaceae, respectively), as well as the *L. philippensis* transcriptome from the PPGPII project, were added to this analysis, in addition to sequences from PlantTribes2 26Gv2.0 scaffold.

Most of the five major clades identified in previous studies [28–31] were strongly supported (bootstrap >70) in both the autotroph-only and autotroph plus parasite *PLL* phylogenetic trees (Figure 1A, Supplemental Figure S2). Genes from all the sampled angiosperms lineages were present in most of the clades. Clade 5, the first distinct monophyletic group (Figure 1A), contains genes from all land plants and is the sister clade to all the others. Clades 4 and 3 form the second main monophyletic group, and are seed plant-wide and eudicot-wide clades, respectively. These two clades share more sequence similarities than the rest and they form a highly supported monophyletic group with two genes from *Selaginella moellendorffii*. A rapid expansion of Clade 4 *PLLs* was observed in most rosid species, but not in other major lineages, including the parasitic plants. In addition, unlike all the other clades where genes from both parasitic Orobanchaceae and *Cuscuta* are present, Clade 4 only has genes from *Striga* and *Triphysaria*. No gene from *Cuscuta* or *Phelipanche* was found in Clade 4. Grouping of Clade 3 and 4 has been observed in McCarthy et al., [29], but not in the other three publications. Clades 1 and 2 form the third major monophyletic group, and each can be further divided into two smaller monophyletic groups, subclades 1-1 and 1-2, and subclades 2-1 and 2-2. Subclades 1-1 and Clade 2 have genes from all the major angiosperm taxa, while Subclade 1-2 contains not only the major angiosperm lineages, but also genes from loblolly pine (*Pinus taeda*), making it a seed plant-wide clade. In the three previous studies that inferred the phylogeny using Neighboring-joining method [28,30,31], Subclade 2-2 was a sister clade to the rest of the Clade 1 plus Clade 2 group from this study, while Subclade 2-1 was classified as a part of Clade 1 (Supplemental Figure S3). Our study provided strong evidence supporting the grouping of the two subclades in Clade 2, a different relationship first revealed by McCarthy et al., 2014 [29].

The haustorial *PLL* genes previously proposed for functional studies from the Yang *et al.,* study were classified into Subclade 1-1 (Supplemental Figure S2 and Supplemental File 1), the largest clade in the *PLL* family. Additionally, these haustorial genes reside on a branch with a longer branch length than most other genes, indicating high sequence divergence in the coding region. Expression analysis from PPGP II transcriptome data (Supplemental Figure S4) revealed that among the four *Triphysaria PLL* genes in Subclade 1-1, *TrVePLL1* is specifically expressed in haustorial stages, which provides stronger support for this gene as a good candidate for functional analysis.

Conserved domain structure among PLL proteins

Domain search results (Figure 1B) showed that all the sequences used for phylogenetic tree inference contain a Pec_lyase_C domain, which carries out the main catalytic function in pectate modification. Subclade 2-2 also contains a unique Pec_lyase_N terminal domain. Based on the inferred protein phylogeny, Subclade 2-2 is an angiosperm-wide group, thus indicating that the Pec_lyase_N terminal domain had evolved or been acquired in a common ancestor of angiosperms. Signal peptides or transmembrane domains were common at the N-terminus of proteins in Clades 1 to 4, but were only found in one gene, *Selmo_v1.0_412910*, in Clade 5 (Supplemental File 2). In some proteins from Subclade 2-1, C-terminus transmembrane domains are detected as well.

An amino acid frequency plot (LOGO) was generated for the Pec_lyase_C domain of each clade for visual comparison (Figure 1C). Clade 5, the sister group to all the other PLLs has an 18 amino acid deletion in addition to other divergent amino acids compared to the other clades. Ca^{2+} binding sites, substrate binding sites, and the active site were predicted based on the literature of PL protein structure [64–67] and these sites are highly conserved among different clades, including the divergent Clade 5.

High sequence divergence and adaptive evolution in parasitic plant PLLs

Long branches, an indication of high sequence divergence, could point to important biological phenomena such as adaptive evolution of the encoded protein, therefore, tests for selective constraints were performed to detect changes in evolutionary pressure within branches housing parasitic plant genes in the *PLL* gene family tree. A branch test was performed using CodeML from the PAML package [52], which compared the foreground parasite *PLL* genes and the background genes from other asterids. Five branches with relaxed purifying selection and one branch with positive selection were detected (Supplemental Table S7). The one branch with positive selection is the branch containing *TrVePLL1*, a gene proposed to be an ideal candidate for functional assays by Yang et al., 2015 [17]. In addition, three out of the five branches with relaxed purifying selection and the *TrVePLL1* branch contain amino acid sites under adaptive evolution in the foreground sequences compared to the background (Supplemental Table S7).

TrVePLL1 is upregulated during haustorium development

TrVeBC3_16311.1, a single *Triphysaria versicolor* gene, was chosen for functional assay and designated as *TrVePLL1.* This gene contains seven exons and six introns, encoding a 1341bp mRNA that translates into a protein containing 466 amino acids (Figure 2A). Similar to other proteins in Subclade 1-1, TrVePLL1 contains 3 functional

motifs, an N-terminal transmembrane domain/ signal peptide, a pectate lyase C domain, and a C-terminus low complexity motif (Figure 2A).

Transcriptome data from PPGP [17] indicated that *TrVePLL1* is upregulated during early haustoria development (stage 3) (Supplemental Figure S4D). To validate the transcriptome results and examine the expression profile of *TrVePLL1* at a finer time scale, the transcript level of *TrVePLL1* was measured from *T. versicolor* roots or haustorial tissues collected at different developmental stages, including 0h, 12h, 24h, 48h, 72h, 5 days, and 10 days post incubation with *M. truncatula* roots (Figure 2B). From 0 to 24 hours post incubation (HPI), the region just behind the root tip starts to become swollen and the epidermal cells grow long haustorial hairs, which adhere to the host root. *TrVePLL1* transcript level increased by 5 times at 24 HPI compared to 0 HPI. From 24 to 72 hours, the haustorium apex grows towards the host root and starts penetration. The transcript level of *TrVePLL1* increased significantly, and reached a plateau (~200 fold higher than 0HPI) at 72 hours after inoculation. At 5 days post inoculation, a mature haustorium is formed with a developed vascular connection. Transcription of *TrVePLL1* remained at a high level five days after inoculation, and decreased at 10 days, when the haustorium was mature [68]. The expression level of *TrVeBC3_3448.1* (*TrVeBC4_p_c2216_g69* in PPGP II assembly), designated as *TrVePLL2*, was also measured in the same tissue as a control. The transcript levels of *TrVePLL2* did not show a significant change post inoculation. The other two *TrVePLLs* in Clade 1-1 were not tested in this experiment, due to very low expression.

Reduction of mature haustorium formation was achieved by knocking down *TrVePLL1* via direct transformation and HIGS

To investigate whether *TrVePLL1* contributes to haustorium formation, gene knockdown assays were carried out with interfering RNA interference (RNAi) delivered using two approaches: transient hairy root transformation in *Triphysaria versicolor*, and host induced gene silencing (HIGS) where the silencing construct is transformed into the host plant.

A 503 base pair sequence from the *TrVePLL1* gene was amplified and cloned into *pHG8-YFP* RNA silencing construct, creating the *pHpTvPLL1* hairpin construct. To prevent off-targeting in both the parasitic plant and the host plant, this fragment was searched against the *T. versicolor* transcriptome assembly and the *Medicago truncatula* genome using BLAST. No perfect matches longer than 20 continuous nucleotides were found in all the three targets. Either the hairpin construct (*pHpTvPLL1*) or the empty construct (*pHG8-YFP*) were transformed into *T. versicolor* and its host plants and the roots were examined for YFP signal (Supplemental Figure S5). Similar transformation efficiencies were observed in the lines with either one of the constructs. On average,

73% and 68% *T. versicolor* root transformed with *pHG8-YFP* and *pHpTvPLL1* constructs, respectively, developed transgenic root expression YFP signals, higher efficiencies than previously reported [33]. Approximately 80% of the *M. truncatula* plants developed transgenic roots in both lines, consistent with previous publications [34]. No morphological difference was observed between roots transformed with the two constructs. The presence of the hairpin construct in *M. truncatula* root expressing YFP was further validated using a polymerase-chain-reaction (Supplemental Figure 6). To obtain enough *T. versicolor* roots for haustorium assay, the transgenic roots were maintained in tissue culture for up to three months with roots trimmed about 1 mm away from the tip periodically to stimulate proliferation. Transgenic roots acquired from the proliferation process retained competency to form haustorium, similar to a non-transformed seedlings at seven days post inoculation (Table 1).

Table 1. Haustorium development in transgenic and non-transgenic T. versicolor roots over time.

Days post inoculation	% of root with haustoria[a]	
	Seedlings	pHG8-YFP
5	83 ± 8 (n=125)	62 ± 11 (n=76)
7	88 ± 4 (n= 117)	83 ± 10 (n=95)

a Value are means ± standard deviation from three biological replicates. Three to five plates were collected for each biological replicate when using seedlings, and each plate contains 10 to 14 roots. Six to eight plates were collected for each replicate when using the transgenic line, and each plate contains three to eight roots with YFP signal. n = the total number of roots in all replicates.

Haustoria were assayed from wild type *Medicago* inoculated with transgenic *T. versicolor*. No morphological differences of the haustoria are observed in the *TrVePLL1* knockdown lines versus the control lines seven days post inoculation. The majority of haustoria are swollen, hairy, and attached to the host root. In the control lines, most haustoria are firmly connected to the host root, namely mature haustoria, while a small percentage (~28%, Figure 3A) are loosely connected and detect readily from the host upon the application of a small mechanical force with forceps. Those loosely connected haustoria were deemed as 'failed haustoria'. A higher percentage (~45%) of failed haustoria was observed in the *TrVePLL1* knockdown lines. To avoid human bias, the treatment types were not known by the researcher when each haustorium was examined. This experiment has been repeated two more times and the same phenomenon was observed (Supplemental Table S5). The same haustoria assay was performed on transgenic *Medicago* inoculated with transgenic *T. versicolor*. Five days post inoculation, about 69% of the *T. versicolor* roots developed mature haustorium when aligned with *M. truncatula* root transformed with the empty vector, and only about

20% of the roots failed to form strong connections (Figure 3C). In the co-culture experiment where the hosts were transformed with *pHpTvPLL1*, 49% of the *T. versicolor* seedlings made mature haustoria, while about 44% of the haustoria were weakly connected (Figure 3C). Overall, the result from HIGS is highly consistent with that obtained from directly transforming the hairpin structure into *T. versicolor*.

To determine whether the increased percentage of failed haustoria is related to the expected decrease in transcript level of *TrVePLL1*, a qRT-PCR assay was conducted. In the wild type host and transgenic parasite co-culture, the transcript level of *TrVePLL1* is the highest in mature haustoria collected from the control group followed by mature haustoria from the knockdown lines (Figure 3B). The failed haustoria from the knock down line transcribed the lowest level of *TrVePLL1*. A similar pattern of transcript level changes was observed in the transgenic host and wild type parasite co-culture. Due to the low number of failed haustoria formed on the control root, this sample was excluded in this experiment. Both mature and failed haustoria attached to the *pHpTvPLL1* root showed decreased transcript abundance of *TrVePLL1* compared to mature haustoria formed on the control root (Figure 3D). Unexpectedly, although the level of expression reduction of the target gene in HIGS is lower than that of direct transformation, the percentage of failed haustorium formed is similar, if not higher.

Staining of haustoria reveals morphological similarities and differences between control and knock down lines

It is difficult to distinguish, through visual inspection of haustorium, the failed from the mature haustoria or the haustorium formed in the knock down lines versus the control lines. In order to observe potential differences in internal haustorium morphology, three staining assays were conducted on haustoria formed from transgenic *Triphysaria versicolor* co-cultured with wild type hosts. The ink-vinegar staining method showed that one to several xylem connections (Figure 4A, B) were observed in *T. versicolor* haustoria formed on *M. truncatula*. More than 70% of the mature haustoria collected developed single or multiple xylem bridges. In the failed haustoria (Figure 4C), only about 50% developed xylem connections (Table 2). Tukey's pairwise using Copenhaver-Holland method showed the difference of % roots with xylem bridge between pHpTvPLL1 mature and failed haustoria is statistically significant ($p<0.05$, Supplemental Table S8). No differences in terms of presence/ absence of xylem bridge or xylem connection number were observed in the *TrVePLL1* knock down line versus the control line (Table 2 and Supplemental Table S8). Compared to the host root (*Arabisopsis thaliana* in this experiment), or other parts of the parasitic plant root, haustorium were stained to a much darker red using Triphenyl tetrazolium chloride (TTC), especially at the host-parasite interface (Figure 4E, F), indicating high metabolic activity. In a few cases, the root tips

were also darker red (Figure 4G). However, no difference was observed between failed versus mature haustoria, or between the *TrVePLL1* knockdown lines and the control lines. Toluidine blue O (TBO), has a high affinity for acidic tissue components and different colors are generated when the dye binds to different components on the cell wall [57]. However, haustorium sections processed from the *TrVePLL1* knock down line and the control line were not visibly different (Figure 4H, I). It's worth mentioning that only mature haustoria were used for sectioning in this study, since failed haustoria detached from the host root during the dehydration and embedding process.

Table 2. Xylem connection observations in transgenic haustoria

Type of haustoria	% roots with xylem bridge[a]	Average number of xylem in a haustorium[b]
pHG8-YFP mature	67 ± 6 (n= 62)	1.32 ± 0.85
pHG8-YFP failed	53 (n= 17)[c]	1.30 ± 0.67
pHpTvPL1 mature	72 ± 8 (n= 46)	1.28 ± 0.79
pHpTvPL1 failed	50 ± 4 (n= 40)	1.15 ± 0.50

a Value are means ± standard deviation from three biological replicates (except for *pHG8-YFP* failed). Three to five plates were collected for each replicate. n = the total number of roots in all replicates.
b only haustorium formed xylem bridge were included in the calculation

Discussion

A robust phylogenetic analysis reveals the evolutionary history of the *PLL* genes.

Compared to the published phylogenetic estimation of the *PLL* gene family [11, 28-31], the result from this research is more thorough and robust. The Bayesian tree constructed by Palusa et al. divided 62 *PLL* proteins from *Arabidopsis thaliana*, *Populus trichocarpa*, and *Oryza sativa* into 3 distinct groups [11]. With rice as the only monocot representative in that study, group II and a few other subgroups were annotated as dicot-specific. However, with increased sampling from diverse monocot species, the phylogeny presented in this research identified monocot genes in these groups. The only true dicot specific clade is Clade 3, which was identified as the *PLL4* subgroup in group I from the Palusa et al. results. McCarthy *et al.* expanded the species list from three to ten and built a high quality phylogeny to infer the ancestry of the *PLL* gene family [29]. The main limitations in the McCarthy *et al*. phylogeny were the lack of resolution between some major clades and the absence of asterid representatives due to the then available

genomes. By sampling a wider range of plant species, and including genes from 8 asterid genomes and transcriptomes, all the clades in this study were resolved into monophyletic groups with strong support, and little ambiguity remaining in terms of the relationship between major clades. There have been other attempts to resolve the phylogeny of PLLs across land plants with a more diverse collection of plant genomes including asterids [30,31]. However, both publications failed to provide supporting evidence for the clade-to-clade relationship as we do in this study.

How does *TrVePLL1* facilitate parasitism? Two hypotheses

In the process of pollen tube growth, pectin deposition and the action of several pectin processing enzymes have been proposed to play essential roles. As a fast growing tissue that penetrates through other plant tissues, the apical cell walls of the pollen tube must be flexible enough to transport and incorporate new cell wall material, and at the same time grow strong enough to withstand turgor pressure [69]. As major cell wall components, pectic molecules have been reported to be actively delivered to the cell wall by vesicles [8,70–72]. Those pectic molecules could either be newly synthesized and delivered from the Golgi body, or recycled from old cell walls that have been degraded by pectic enzymes [9]. On the other hand, pectate lyase-like proteins have also been proposed to loosen the cell wall of the stylar cells, thus facilitating pollen tube penetration [9].

Haustorium penetration, which is morphologically very similar to the process of pollen tube growth, could have adapted a similar molecular mechanism. In fact, some *PLLs* in the parasitic Orobanchaceae were derived from genes formerly expressed in floral tissues of non-parasitic relatives [17]. In addition, Losner-Goshen *et al.* used immunolabeling of specific pectin antibodies and observed the disappearance of pectins from the cell walls of sunflower root at the interface of parasite-host interaction [73]. Taken together, we propose two possible mechanisms for how *TrVePLL1* is involved in haustorium growth. *Hypothesis 1*: *TrVePLL1* facilitates the mobilization of pectin molecules by degrading demethylated pectin from old parasite cell walls, and using the degradation products as building material for the new walls that grow at the apical tip of the haustorium. *Hypothesis 2*: *TrVePLL1* facilitates haustorium penetration in the host tissue by degrading pectin located either in the host cell wall or in the host middle lamella. To further test these two hypotheses, additional experiments, such as detecting pectin contents using electron microscopy or tracing the movement of the TrVePLL1 protein at high-resolution, are needed.

Working towards durable resistance in a changing environment

Despite the high heterozygosity level of gene sequences in the obligate outcrossing species *Triphysaria versicolor*, the success of the knockdown experiments in this study to affect haustorial development is encouraging. More importantly, the success of using host induced gene silencing (HIGS) to influence haustorium development shed lights on the potential of novel parasitic plant management practices in the weedy parasites, such as *Striga*. Functions of orthologs of *TrVePLL1* in the two *Striga* species (designated as *StHePLL1* and *StAsPLL1*) should be tested if genetic manipulation becomes feasible. *StHePLL1* is of special interest, not only because of its high sequence divergence (reflected by the long branch length in Supplemental Figure S2) and high expression level in haustorial stages [17], but also because it can be a candidate gene for parasitic weed control. However, as genetically divergent plants, some parasites could overcome the effect of HIGS quickly if only one gene is targeted. A multi-targeted HIGS approach was proposed by Dr. Jonathan Gressel, in which RNAi constructs targeting many haustorially expressed, parasitism related genes can be "stacked" into the host [74]. To fulfill this goal, more functional characterization studies like the experiment conducted in this research needs to be executed to generate a good set of target genes.

Another limitation of targeting a single gene is the potential gene redundancy effect achieved by other paralogous members sharing a similar function. For instance, 27 *PLL* genes were identified in *T. versicolor* in this study. Out of the 27 *PLLs*, five are significantly differentially expressed in haustorial stages, and another seven have their highest expression levels in haustorial stages (Supplemental Figure S7). Although *TrVePLL1* has several unique features that qualify it as a good candidate for functional assay, its function could have been complemented by other *PLLs*, thus resulting in over 50% mature and strongly connected haustoria. To tackle this limitation, either silencing constructs that can target multiple candidate genes must be designed, and/or the 'stacked' gene silencing approach as mentioned above, could eventually be pursued.

Conclusions

Our results provide novel insights into the evolutionary history of the pectate lyase like genes in land plants, as well as evidence of the involvement of *TrVePLL1* in haustorium development in parasitic Orobanchaceae. The *PLL* gene family tree, constructed using sequences from 34 plant species representing major groups of land plants, including six parasitic plants, and one carnivorous plant, *Utricularia*, revealed new relationships of the five major clades with strong supporting evidence. *TrVePLL1*, a *Triphysaria versicolor* gene predicted to be involved in parasitism [17], was the only haustorial-specific gene in Subclade 1-1. Furthermore, parasitic plant genes in the

branch housing *TrVePLL1* showed signatures of positive selection. Collectively, this evidence supported *TrVePLL1* as a strong candidate gene for functional assays. Knocking down the expression level of *TrVePLL1* by transforming *T. versicolor* root with an antisense hairpin construct, or via host-induced gene silencing (HIGS), reduced the percentage of mature haustorium formation. This study is the first to provide experimental evidence that a cell wall processing enzyme plays a crucial role in haustorium development. With rapid advancements in genome and transcriptomic sequencing technologies and data processing methodologies, scientists are well-equipped to identify more candidate genes potentially related to parasitism. However, functional characterization of those genes remains a challenge. Further research like this study is needed to fully understand their roles and to explore new strategies for disrupting parasitic mechanisms.

References

1. Ridley BL, O'Neill MA, Mohnen D. Pectins: structure, biosynthesis, and oligogalacturonide-related signaling. Phytochemistry. 2001;57: 929–967.

2. Eticha D, Stass A, Horst WJ. Cell-wall pectin and its degree of methylation in the maize root-apex: significance for genotypic differences in aluminium resistance. Plant Cell Environ. 2005;28: 1410–1420.

3. Starr MP, Moran F. Eliminative split of pectic substances by phytopathogenic soft-rot bacteria. Science. 1962;135: 920–921.

4. Collmer A, Keen NT. The role of pectic enzymes in plant pathogenesis. 1986. doi:10.1146/annurev.py.24.090186.002123

5. Nakajima N, Ishihara K, Tanabe M, Matsubara K, Matsuura Y. Degradation of pectic substances by two pectate lyases from a human intestinal bacterium, Clostridium butyricum-beijerinckii group. J Biosci Bioeng. 1999;88: 331–333.

6. Kotoujansky A. Molecular Genetics of Pathogenesis by Soft-Rot Erwinias. Annu Rev Phytopathol. 1987;25: 405–430.

7. Ohtsuki T, Taniguchi Y, Kohno K, Fukuda S, Usui M, Kurimoto M. Cry j 2, a major allergen of Japanese cedar pollen, shows polymethylgalacturonase activity. Allergy. 1995;50: 483–488.

8. Ischebeck T, Stenzel I, Heilmann I. Type B phosphatidylinositol-4-phosphate 5-kinases mediate Arabidopsis and Nicotiana tabacum pollen tube growth by regulating apical pectin secretion. Plant Cell. 2008;20: 3312–3330.

9. Wu Y, Qiu X, Du S, Erickson L. PO149, a new member of pollen pectate lyase-like

gene family from alfalfa. Plant Mol Biol. 1996;32: 1037–1042.

10. Jiang J, Yao L, Yu Y, Liang Y, Jiang J, Ye N, et al. PECTATE LYASE-LIKE 9 from Brassica campestris is associated with intine formation. Plant Sci. 2014;229: 66–75.

11. Palusa S, Golovkin M, Shin S, Richardson DN, Reddy ASN. Organ-specific, developmental, hormonal and stress regulation of expression of putative pectate lyase genes in Arabidopsis. New Phytol. 2007;174: 537–550.

12. Uluisik S, Seymour GB. Pectate lyases: Their role in plants and importance in fruit ripening. Food Chem. 2020;309: 125559.

13. Sun H, Hao P, Gu L, Cheng S, Wang H, Wu A, et al. Pectate lyase-like Gene GhPEL76 regulates organ elongation in Arabidopsis and fiber elongation in cotton. Plant Sci. 2020;293: 110395.

14. Xu Z, Dai J, Kang T, Shah K, Li Q, Liu K, et al. PpePL1 and PpePL15 Are the Core Members of the Pectate Lyase Gene Family Involved in Peach Fruit Ripening and Softening. Front Plant Sci. 2022;13: 844055.

15. Yang L, Huang W, Xiong F, Xian Z, Su D, Ren M, et al. Silencing of SlPL, which encodes a pectate lyase in tomato, confers enhanced fruit firmness, prolonged shelf-life and reduced susceptibility to grey mould. Plant Biotechnol J. 2017;15: 1544–1555.

16. Cui S, Wakatake T, Hashimoto K, Saucet SB, Toyooka K, Yoshida S, et al. Haustorial Hairs Are Specialized Root Hairs That Support Parasitism in the Facultative Parasitic Plant Phtheirospermum japonicum. Plant Physiol. 2016;170: 1492–1503.

17. Yang Z, Wafula EK, Honaas LA, Zhang H, Das M, Fernandez-Aparicio M, et al. Comparative transcriptome analyses reveal core parasitism genes and suggest gene duplication and repurposing as sources of structural novelty. Mol Biol Evol. 2015;32: 767–790.

18. Yoshida S, Cui S, Ichihashi Y, Shirasu K. The Haustorium, a Specialized Invasive Organ in Parasitic Plants. Annu Rev Plant Biol. 2016;67: 643–667.

19. Leso M, Kokla A, Feng M, Melnyk CW. Pectin modifications promote haustoria development in the parasitic plant Phtheirospermum japonicum. Plant Physiol. 2023;194: 229–242.

20. Dixit S, Upadhyay SK. Melting the wall: plant parasitism entails pectin modification. Plant Signal Behav. 2023;18: 2252219.

21. Jhu M-Y, Ichihashi Y, Farhi M, Wong C, Sinha NR. LATERAL ORGAN

BOUNDARIES DOMAIN 25 functions as a key regulator of haustorium development in dodders. Plant Physiol. 2021;186: 2093–2110.

22. Kurotani K-I, Wakatake T, Ichihashi Y, Okayasu K, Sawai Y, Ogawa S, et al. Host-parasite tissue adhesion by a secreted type of β-1,4-glucanase in the parasitic plant Phtheirospermum japonicum. Commun Biol. 2020;3: 407.

23. Jhu M-Y, Farhi M, Wang L, Zumstein K, Sinha NR. Investigating Host and Parasitic Plant Interaction by Tissue-Specific Gene Analyses on Tomato and Cuscuta campestris Interface at Three Haustorial Developmental Stages. Front Plant Sci. 2021;12: 764843.

24. Bradley JM, Butlin RK, Scholes JD. Comparative secretome analysis of Striga and Cuscuta species identifies candidate virulence factors for two evolutionarily independent parasitic plant lineages. BMC Plant Biol. 2024;24: 251.

25. Bawin T, Didriksen A, Faehn C, Olsen S, Sørensen I, Rose JKC, et al. Cuscuta campestris fine-tunes gene expression during haustoriogenesis as an adaptation to different hosts. Plant Physiol. 2023;194: 258–273.

26. Fernández-Aparicio M, Delavault P, Timko MP. Management of Infection by Parasitic Weeds: A Review. Plants. 2020;9. doi:10.3390/plants9091184

27. Zhang H. Phylogenetic and functional studies on parasitism genes in Orobanchaceae and Convolvulaceae. dePamphilis C, editor. Ph.D, The Pennsylvania State University. 2020. Available: https://search.proquest.com/openview/be0f185db348e0573dc527fc9fb57397/1?pq-origsite=gscholar&cbl=18750&diss=y

28. Sun L, van Nocker S. Analysis of promoter activity of members of the PECTATE LYASE-LIKE (PLL) gene family in cell separation in Arabidopsis. BMC Plant Biol. 2010;10: 152.

29. McCarthy TW, Der JP, Honaas LA, dePamphilis CW, Anderson CT. Phylogenetic analysis of pectin-related gene families in Physcomitrella patensand nine other plant species yields evolutionary insights into cell walls. BMC Plant Biol. 2014;14: 1–14.

30. Zheng Y, Yan J, Wang S, Xu M, Huang K, Chen G, et al. Genome-wide identification of the pectate lyase-like (PLL) gene family and functional analysis of two PLL genes in rice. Mol Genet Genomics. 2018;293: 1317–1331.

31. Sun H, Hao P, Ma Q, Zhang M, Qin Y, Wei H, et al. Genome-wide identification and expression analyses of the pectate lyase (PEL) gene family in cotton (Gossypium hirsutum L.). BMC Genomics. 2018;19: 661.

32. Tomilov A, Tomilova N, Yoder JI. Agrobacterium tumefaciens and Agrobacterium

rhizogenes transformed roots of the parasitic plant Triphysaria versicolor retain parasitic competence. Planta. 2006;225: 1059–1071.

33. Bandaranayake PCG, Filappova T, Tomilov A, Tomilova NB, Jamison-McClung D, Ngo Q, et al. A single-electron reducing quinone oxidoreductase is necessary to induce haustorium development in the root parasitic plant Triphysaria. The Plant Cell Online. 2010;22: 1404–1419.

34. Bandaranayake PC, Yoder JI. Trans-specific gene silencing of acetyl-CoA carboxylase in a root-parasitic plant. Mol Plant Microbe Interact. 2013;26: 575–584.

35. Wafula EK, Zhang H, Von Kuster G, Leebens-Mack JH, Honaas LA, dePamphilis CW. PlantTribes2: Tools for comparative gene family analysis in plant genomics. Front Plant Sci. 2022;13: 1011199.

36. The Galaxy Community. The Galaxy platform for accessible, reproducible and collaborative biomedical analyses: 2022 update. Nucleic Acids Res. 2022;50: W345–W351.

37. Zhang H, Wafula EK, Eilers J, Harkess AE, Ralph PE, Timilsena PR, et al. Building a foundation for gene family analysis in Rosaceae genomes with a novel workflow: A case study in Pyrus architecture genes. Front Plant Sci. 2022;13: 975942.

38. Haas BJ. Transdecoder. In: GitHub [Internet]. 2024 [cited 2024]. Available: https://github.com/TransDecoder/TransDecoder

39. Camacho C, Coulouris G, Avagyan V, Ma N, Papadopoulos J, Bealer K, et al. BLAST+: architecture and applications. BMC Bioinformatics. 2009;10: 421.

40. Eddy SR. Accelerated Profile HMM Searches. PLoS Comput Biol. 2011;7: e1002195.

41. Katoh K, Misawa K, Kuma K, Miyata T. MAFFT: a novel method for rapid multiple sequence alignment based on fast Fourier transform. Nucleic Acids Res. 2002;30: 3059–3066.

42. Capella-Gutiérrez S, Silla-Martínez JM, Gabaldón T. trimAl: a tool for automated alignment trimming in large-scale phylogenetic analyses. Bioinformatics. 2009;25: 1972–1973.

43. Stamatakis A. RAxML version 8: a tool for phylogenetic analysis and post-analysis of large phylogenies. Bioinformatics. 2014;30: 1312–1313.

44. Minh BQ, Schmidt HA, Chernomor O, Schrempf D, Woodhams MD, von Haeseler A, et al. IQ-TREE 2: New Models and Efficient Methods for Phylogenetic Inference in the Genomic Era. Mol Biol Evol. 2020;37: 1530–1534.

45. Minh BQ, Nguyen MAT, von Haeseler A. Ultrafast approximation for phylogenetic bootstrap. Mol Biol Evol. 2013;30: 1188–1195.

46. Stanke M, Steinkamp R, Waack S, Morgenstern B. AUGUSTUS: a web server for gene finding in eukaryotes. Nucleic Acids Res. 2004;32: W309–12.

47. Jones P, Binns D, Chang H-Y, Fraser M, Li W, McAnulla C, et al. InterProScan 5: genome-scale protein function classification. Bioinformatics. 2014;30: 1236–1240.

48. Almagro Armenteros JJ, Tsirigos KD, Sønderby CK, Petersen TN, Winther O, Brunak S, et al. SignalP 5.0 improves signal peptide predictions using deep neural networks. Nat Biotechnol. 2019;37: 420–423.

49. Krogh A, Larsson B, von Heijne G, Sonnhammer EL. Predicting transmembrane protein topology with a hidden Markov model: application to complete genomes. J Mol Biol. 2001;305: 567–580.

50. Crooks GE, Hon G, Chandonia J-M, Brenner SE. WebLogo: a sequence logo generator. Genome Res. 2004;14: 1188–1190.

51. Gao F, Chen C, Arab DA, Du Z, He Y, Ho SYW. EasyCodeML: A visual tool for analysis of selection using CodeML. Ecol Evol. 2019;9: 3891–3898.

52. Yang Z. PAML 4: phylogenetic analysis by maximum likelihood. Mol Biol Evol. 2007;24: 1586–1591.

53. Yang Z, Wong WSW, Nielsen R. Bayes empirical bayes inference of amino acid sites under positive selection. Mol Biol Evol. 2005;22: 1107–1118.

54. Bandaranayake PCG, Yoder JI. Factors affecting the efficiency of Rhizobium rhizogenes root transformation of the root parasitic plant Triphysaria versicolor and its host Arabidopsis thaliana. Plant Methods. 2018;14: 61.

55. Boisson-Dernier A, Chabaud M, Garcia F, Bécard G, Rosenberg C, Barker DG. Agrobacterium rhizogenes-transformed roots of Medicago truncatula for the study of nitrogen-fixing and endomycorrhizal symbiotic associations. Mol Plant Microbe Interact. 2001;14: 695–700.

56. Stūrīte I, Henriksen TM, Breland TA. Distinguishing between metabolically active and inactive roots by combined staining with 2,3,5-triphenyltetrazolium chloride and image colour analysis. Plant Soil. 2005;271: 75–82.

57. Pradhan Mitra P, Loqué D. Histochemical staining of Arabidopsis thaliana secondary cell wall elements. J Vis Exp. 2014. doi:10.3791/51381

58. Porter RH, Durrell M, Romm HJ. The Use of 2,3,5-Triphenyl-Tetrazoliumchloride as a Measure of Seed Germinability. Plant Physiol. 1947;22: 149–159.

59. Vierheilig H, Coughlan AP, Wyss U, Piche Y. Ink and vinegar, a simple staining technique for arbuscular-mycorrhizal fungi. Appl Environ Microbiol. 1998;64: 5004–5007.

60. Untergasser A, Cutcutache I, Koressaar T, Ye J, Faircloth BC, Remm M, et al. Primer3—new capabilities and interfaces. Nucleic Acids Res. 2012;40: e115–e115.

61. Koressaar T, Remm M. Enhancements and modifications of primer design program Primer3. Bioinformatics. 2007;23: 1289–1291.

62. Hoshino A, Jayakumar V, Nitasaka E, Toyoda A, Noguchi H, Itoh T, et al. Genome sequence and analysis of the Japanese morning glory Ipomoea nil. Nat Commun. 2016;7: 13295.

63. Wu S, Lau KH, Cao Q, Hamilton JP, Sun H, Zhou C, et al. Genome sequences of two diploid wild relatives of cultivated sweetpotato reveal targets for genetic improvement. Nat Commun. 2018;9: 4580.

64. PMR6, a Pectate Lyase–Like Gene Required for Powdery Mildew Susceptibility in Arabidopsis. Available: https://academic.oup.com/plcell/article-abstract/14/9/2095/6009825

65. Leng Y, Yang Y, Ren D, Huang L, Dai L, Plant … W-Y. A rice PECTATE LYASE-LIKE gene is required for plant growth and leaf senescence. 2017. doi:10.1104/pp.16.01625 PMID - 28455404

66. Scavetta RD, Herron SR, Hotchkiss AT, Kita N, Keen NT, Benen JAE, et al. Structure of a Plant Cell Wall Fragment Complexed to Pectate Lyase C. Plant Cell. 1999;11: 1081–1092.

67. Yoder MD, Jurnak F. The Refined Three-Dimensional Structure of Pectate Lyase C from Erwinia chrysanthemi at 2.2 Angstrom Resolution (Implications for an Enzymatic Mechanism). Plant Physiol. 1995;107: 349–364.

68. Westwood JH, dePamphilis CW, Das M, Fernández-Aparicio M, Honaas LA, Timko MP, et al. The Parasitic Plant Genome Project: New Tools for Understanding the Biology of Orobanche and Striga. Weed Sci. 2012;60: 295306.

69. Gaffe J, Tieman DM, Handa AK. Pectin Methylesterase Isoforms in Tomato (Lycopersicon esculentum) Tissues (Effects of Expression of a Pectin Methylesterase Antisense Gene). Plant Physiol. 1994;105: 199–203.

70. Heslop-Harrison J, Heslop-Harrison Y. The growth of the grass pollen tube: 1. Characteristics of the polysaccharide particles (“P-particles”) associated with apical growth. Protoplasma. 1982;112: 71–80.

71. Rosen WG, Gawlik SR. Fine structure of lily pollen tubes following various fixation

and staining procedures. Protoplasma. 1966;61: 181–191.

72. Dashek WV, Rosen WG. Electron microscopical localization of chemical components in the growth zone of lily pollen tubes. Protoplasma. 1966;61: 192–204.

73. Losner-Goshen D, Portnoy VH, Mayer AM, Joel DM. Pectolytic Activity by the Haustorium of the Parasitic PlantOrobancheL. (Orobanchaceae) in Host Roots. Ann Bot. 1998;81: 319–326.

74. Gressel J, Gassmann AJ, Owen MD. How well will stacked transgenic pest/herbicide resistances delay pests from evolving resistance? Pest Manag Sci. 2017;73: 22–34.

Figure caption

Figure 1. Phylogeny and domain structures of pectate lyase like (PLL) genes across land plants. (A). Simplified phylogenetic tree of the *PLL* gene family constructed with IQtree. Monophyletic groups were represented with triangles and colored according to the range of species present in the clade. Blue: Angiosperm only; Green: Seed plant (Angiosperm + Pine); Salmon: Eudicot only; Yellow: Land plant wide; Black: others. Numbers at nodes are bootstrap values. Arabidopsis genes housed in each clade are listed in the parentheses following the clade name along with abbreviations of parasites (Ca: *Cuscuta australis*; Cc: *Cuscuta campestris*; Pa: *Phelipanche aegyptiaca*; Sa: *Striga asiatica*; Sh: *Striga hermonthica*; Tv: *Triphysaria versicolor*). Numbers at the nodes are bootstraps values, where the number before '/' is value from tree constructed with only autotrophic plant and the number after is value from tree constructed with both autotrophic and parasitic plant. The list of plants used for the analysis is available in Supplemental Figure S1. (B). Domain structure of proteins in each clade. (C). LOGO plot showing a comparison of amino acid frequency at equivalent positions of the Pec_layse_C domain among the seven major clades and subclades. Arrows above the image indicate functional residues predicted based on published PLL protein structure from previous studies.

Figure 2. Gene model of *TrVePLL1* and its expression levels during haustorium development in *Triphysaria versicolor*. (A). The seven exons (Blue box) transcribe into a 1341nt mRNA, which translates into the TrVePLL1 protein that contains three predicted functional domains: a signal peptide (Orange), a Pec_lyase_C domain (Pink), and a low complexity domain (Purple). (B). Haustorium development from 0 hour post inoculation till maturation (120 HPI, hours post inoculation) and relative transcript level of *TrVePLL1* and *TrVePLL2*. Total RNA of three biological replicates each consisting of haustoria from 6-8 plants were used for qRT-PCR. Note the log scale y axis.

Figure 3. Haustorium formation rate and haustorium categorization in different co-culture experiments and quantification of *TrVePLL1* transcript level. *pHpTvPLL1* and the control vector *pHG8-YFP* were transformed to *Triphysaria* root (A) or *Medicago* root (C) using a hairy root transformation system. Five biological replicates were used in (A) and (C). 50 to 60 transformed roots from 8-10 independent *Triphysaria* root cultures were analyzed in each biological replicate in (A). 80-100 wild type *Triphysaria* seedlings were co-cultured with 8-10 transformed *Medicago* roots in each replicate in (C). **$P < 0.01$. (B) and (D) show steady state transcript levels of *TrVePLL1* determined by qRT-PCR and normalized to the constitutively expressed gene *TrVePP2A*. 8 to10 haustoria were collected for each biological replicate and three biological replicates were generated for each treatment. Expression levels of *TrVePLL1* in *pHpTvPLL1* mature

were set as 1. Levels of significance were calculated using the Mann-Whitney-Wilcoxon (MWW) test. Note that no qRT-PCR was performed on failed haustorium from wild-type *Triphasaria* co-cultured with *Medicago* roots transformed with *pHpTvPLL1* due to the small amount of failed haustoria collected from this co-culture experiment.

Figure 4. Morphological differences and similarities between haustorium formed by transgenic *Triphysaria* roots. (A)-(D): Ink and vinegar stained haustoria at 7 days post inoculation (DPI), showing difference in xylem connection. (E)-(G): Tetrazolium stained haustoria at 7 DPI. (E) and (F) showing a darker color in the parasite root, especially near the haustorial apex. (G) showed color accumulation at the parasite root tip.
(H) and (I): 7 DPI haustorium sections stained with Toluidine blue O (TBO) .
(A), (C), (D), (F), (I) were collected from plants transformed with the hairpin construct, pHpTvPL1, whereas (B), (E), (G) and (H) were collected from plants transformed with the control vector, pHG8-YFP.

Supplemental Figure S1. Species tree of sampled plant taxa in the phylogenetic study. * indicating parasitic plant species used in the research. Green box presented an alternative species relationship in the Orobanchaceae family, the common ancestor of which was marked with a yellow star. Different colors represent different major land plant groups. Green: asterid; Red: Rosid; Purple: Basal eudicot; Yellow: Monocots; Blue: Basal angiosperm and gymnosperm; Black: Lycophyte and Moss.

Supplemental Figure S2. Phylogenetic trees of the PLL gene family constructed with only autotrophic plant PLL genes using IQtree (A) or RAxML (B) and with PLL genes from both autotrophic and parasitic plants using IQtree (C) or RAxML (D). Different colors represent different major land plant groups. Green: asterid; Red: Rosid; Purple: Basal eudicot; Yellow: Monocots; Blue: Basal angiosperm and gymnosperm; Black: Lycophyte and Moss.

Supplemental Figure S3. Comparison of PLL gene family trees and gene family analysis methods from various publications and this work. (A) Phylogeny from Sun and van Nocker, 2010; (B) Simplified phylogeny from McCarthy et al., 2014; (C) Simplified phylogeny from Sun et al., 2018; (D) Simplified phylogeny from Zheng et al., 2018; and (E) Simplified phylogeny from this work. (F) Summary and comparison of gene family analysis methods from the selected publications. Phylogenies in (B) to (E) are simplified to only show the overall structure with Arabidopsis genes for comparison purposes. Bootstrap (bs) values at the nodes represent the bs value of the largest monophyletic group housing the Arabidopsis genes shown at the tip. Colored backgrounds indicate

clades identified by the Sun and van Nocker, 2010 work, whereas clades on the right side of each phylogeny shows the corresponding clades identified by this study.

Supplemental Figure S4. Normalized transcript level (TPM) of *T. versicolor* genes from *PLL* Subclass 1-1. Triplicated PPGP II transcript data was used for (A) to (C), and PPGP I transcript data was used for (D). X axis showing developmental stages (Stage abbreviated as S in the x axis legend). Blue boxes highlighting haustorial stages.

Supplemental Figure S5. *Triphysaria versicolor* (A-F) and *Medicago truncatula* (G-J) transformed with pHG8-YFP. (A), (C), (D), (E), (G), and (I) are epifluorescence photos showing YFP expression. (B), (F), (H), and (J) are bright field photos. (A) and (B) showing a callus expressing YFP signal 2 weeks post *Agrobacterium* inoculation. (C) showing a single root developed from the transgenic callus 3 weeks post *Agrobacterium* inoculation. (D) showing transgenic root proliferation after removing root tip. (E) and (F) showing transgenic Triphysaria root forming haustorium on *Medicago* root 5 days post co-culture. (G) and (F) showing 6 week old transgenic *Medicago* root without parasitization by *Triphysaria*. (I) and (J) are *Triphysaria* roots making haustorium on transgenic *Medicago* roots. C: callus; T: *Triphysaria versicolor* root; M: *Medicago truncatula* root; H: haustorium. Bar: 1mm, unless otherwise indicated.

Supplemental Figure S6. Polymerase chain reaction of TrVePLL1 using DNA from *Medicago* roots. TY: transgenic root showing YFP signal; TnY: transgenic root not showing YFP signal; P: positive control, in which the *pHpTvPLL1* construct was used as template; NTC: no template control; nT: non transgenic root. Ladder: from the top to bottom band size: 650bp, 500bp, 400bp, 300bp, 200bp, 100bp.

Supplemental Figure S7. A heat map showing the expression level of all *T. versicolor* PLL genes. Blue star on the right indicates this gene is differentially expressed in haustorial tissues. Yellow star on the right indicates the highest expression level of this gene is found in haustorial tissues.

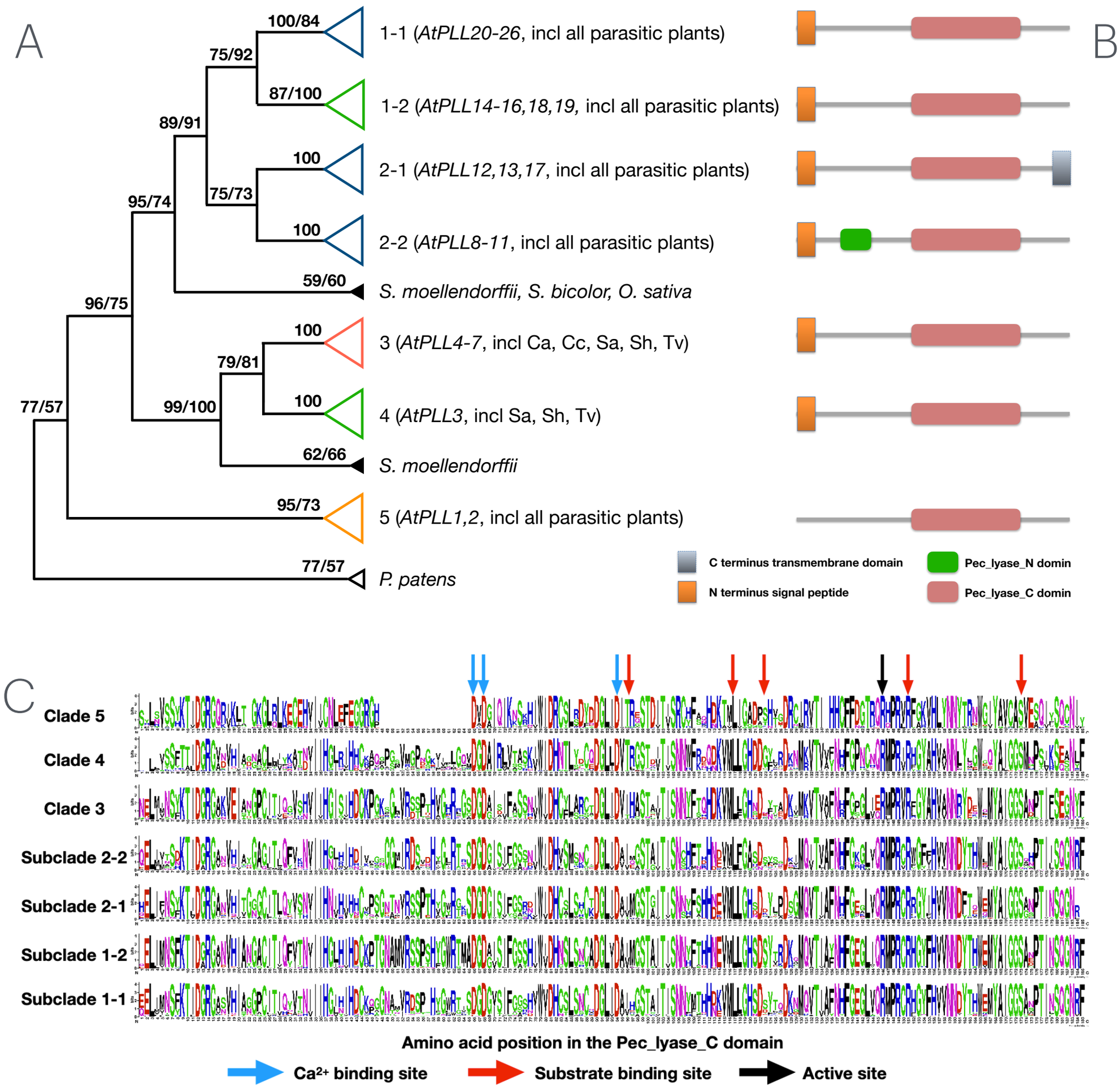
A
B
C
100/84
75/92
87/100
89/91
100
75/73
95/74
100
59/60
96/75
100
79/81
77/57
99/100
100
62/66
95/73
77/57
1-1 (AtPLL20-26, incl all parasitic plants)
1-2 (AtPLL14-16,18,19, incl all parasitic plants)
2-1 (AtPLL12,13,17, incl all parasitic plants)
2-2 (AtPLL8-11, incl all parasitic plants)
S. moellendorffii, S. bicolor, O. sativa
3 (AtPLL4-7, incl Ca, Cc, Sa, Sh, Tv)
4 (AtPLL3, incl Sa, Sh, Tv)
S. moellendorffii
5 (AtPLL1,2, incl all parasitic plants)
P. patens
C terminus transmembrane domain
N terminus signal peptide
Pec_lyase_N domin
Pec_lyase_C domin
Clade 5
Clade 4
Clade 3
Subclade 2-2
Subclade 2-1
Subclade 1-2
Subclade 1-1
Amino acid position in the Pec_lyase_C domain
Ca2+ binding site
Substrate binding site
Active site

A

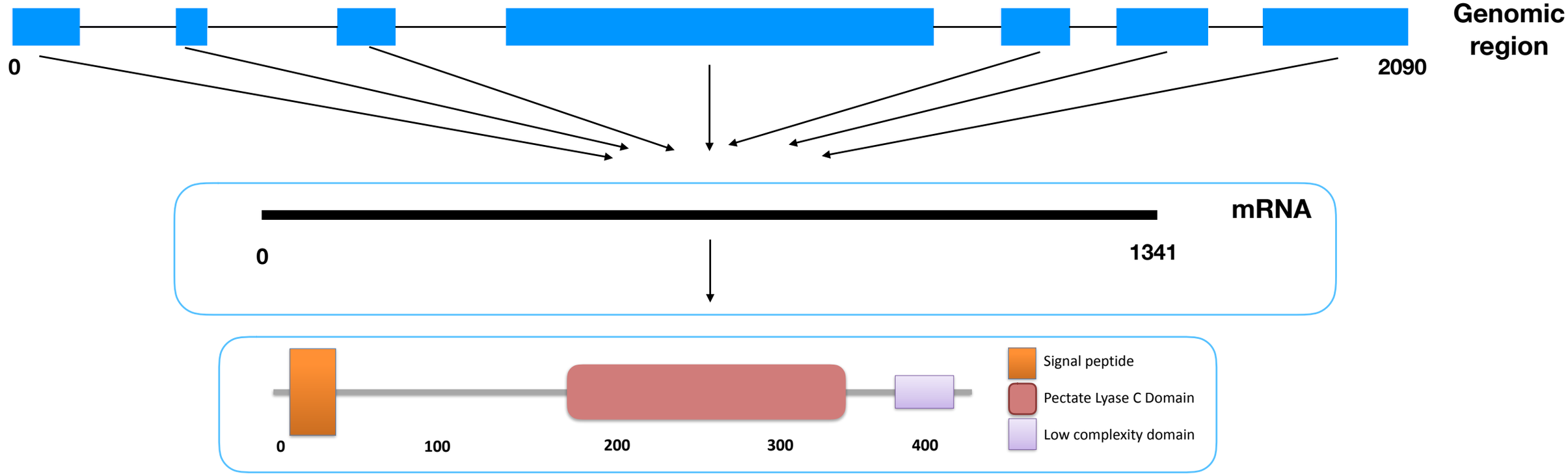
Genomic region
0
2090
mRNA
0
1341
0
100
200
300
400
Signal peptide
Pectate Lyase C Domain
Low complexity domain

B

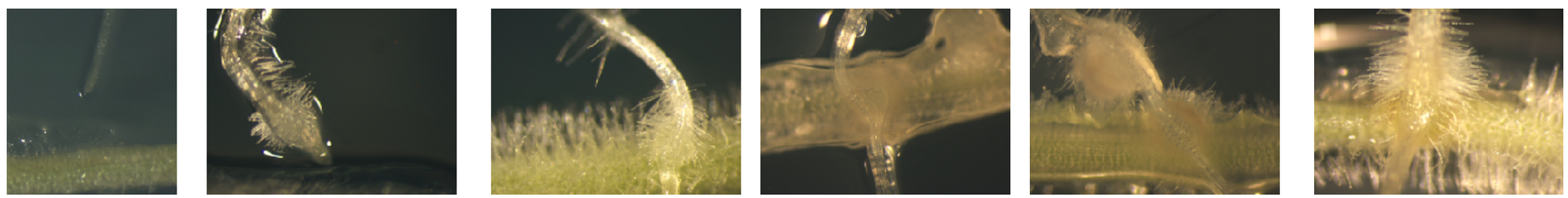

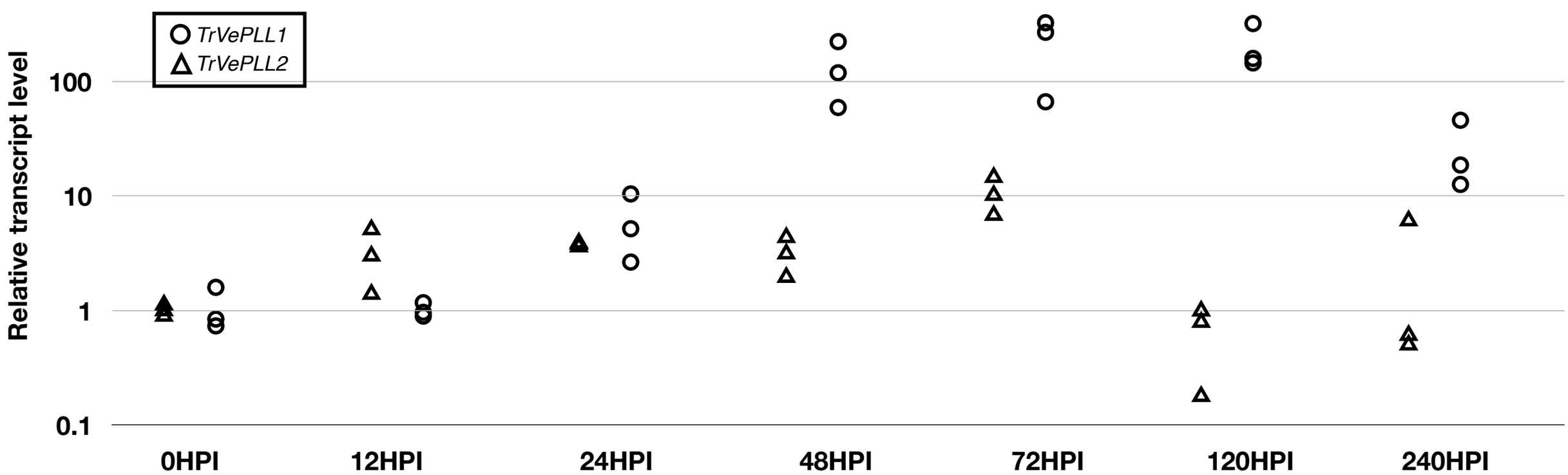
TrVePLL1
TrVePLL2
Relative transcript level
100
10
1
0.1
0HPI
12HPI
24HPI
48HPI
72HPI
120HPI
240HPI

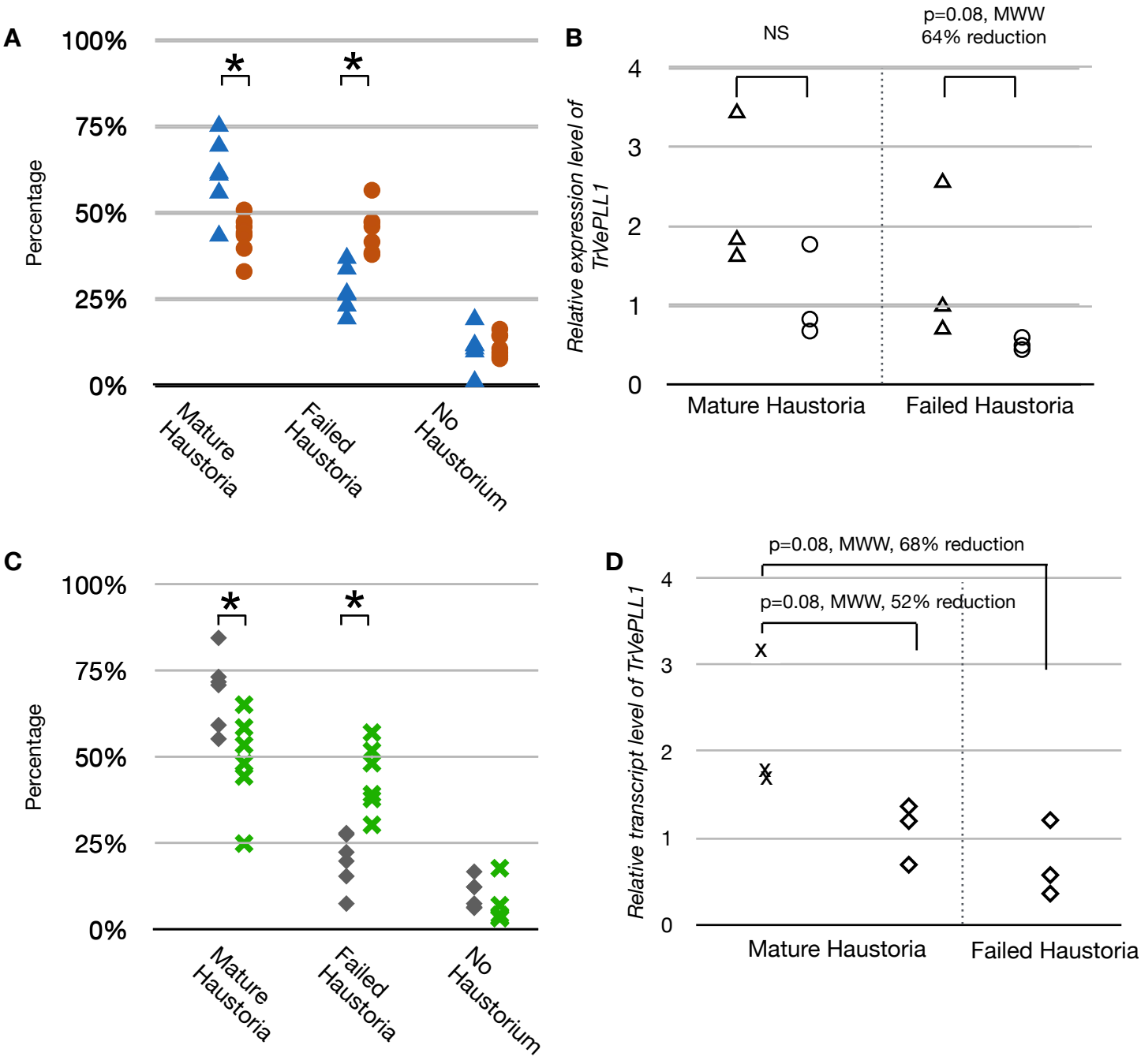
A
100%
75%
50%
25%
0%
Percentage
*
*
Mature Haustoria
Failed Haustoria
No Haustorium
B
NS
p=0.08, MWW
64% reduction
Relative expression level of TrVePLL1
4
3
2
1
0
Mature Haustoria
Failed Haustoria
C
100%
75%
50%
25%
0%
Percentage
*
*
Mature Haustoria
Failed Haustoria
No Haustorium
D
p=0.08, MWW, 68% reduction
p=0.08, MWW, 52% reduction
Relative transcript level of TrVePLL1
4
3
2
1
0
Mature Haustoria
Failed Haustoria
pHpTvPLL1 in T. versicolor
pHG8-YFP in T. versicolor
pHpTvPLL1 in M. truncatula
pHG8-YFP in M. truncatula

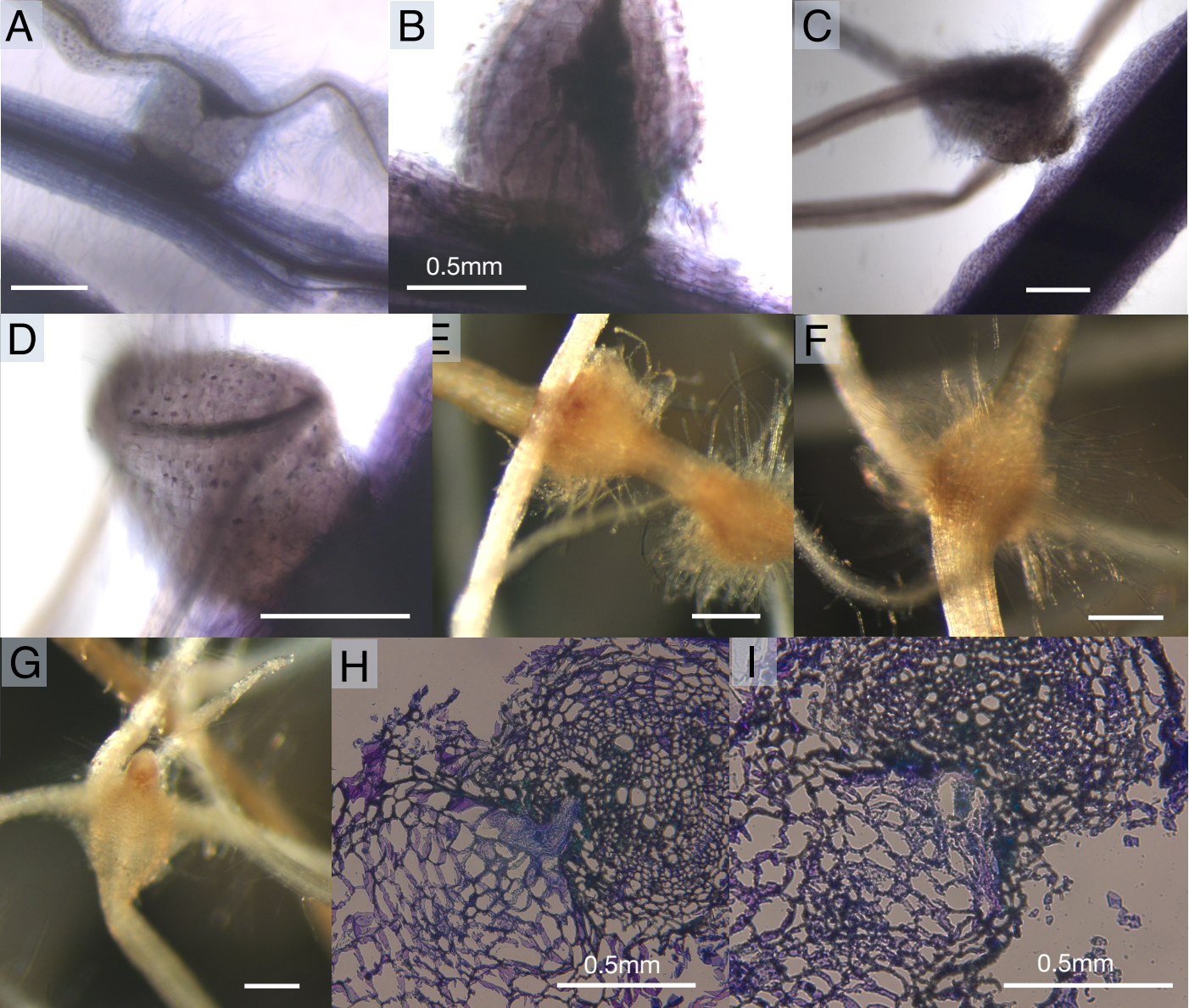
A
B
0.5mm
C
D
E
F
G
H
0.5mm
I
0.5mm